scientific reports

Check for updates

OPEN

# The metabolic clock of ketamine abuse in rats by a machine learning model

Tao Wang[1,2,3,5], Qian Zheng[1,2,3,5], Qian Yang[1,2,3], Fang Guo[1,2,3], Haiyan Cui[1,2,3], Meng Hu[1,2,3], Chao Zhang[1,2,3], Zhe Chen[1,2,3], Shanlin Fu[1,4], Zhongyuan Guo[1,2,3]✉, Zhiwen Wei[1,2,3]✉ & Keming Yun[1,2,3]✉

**Ketamine has recently become an anesthetic drug used in human and veterinary clinical medicine for illicit abuse worldwide, but the detection of illicit abuse and inference of time intervals following ketamine abuse are challenging issues in forensic toxicological investigations. Here, we developed methods to estimate time intervals since ketamine use is based on significant metabolite changes in rat serum over time after a single intraperitoneal injection of ketamine, and global metabolomics was quantified by ultra-performance liquid chromatography-quadrupole-time-of-flight mass spectrometry (UPLC-Q-TOF–MS). Thirty-five rats were treated with saline (control) or ketamine at 3 doses (30, 60, and 90 mg/kg), and the serum was collected at 21 time points (0 h to 29 d). Time-dependent rather than dose-dependent features were observed. Thirty-nine potential biomarkers were identified, including ketamine and its metabolites, lipids, serotonin and other molecules, which were used for building a random forest model to estimate time intervals up to 29 days after ketamine treatment. The accuracy of the model was 85.37% in the cross-validation set and 58.33% in the validation set. This study provides further understanding of the time-dependent changes in metabolites induced by ketamine abuse.**

**Keywords** Ketamine, Inference of time interval, Metabolomics, Drug abuse, Machine learning

Ketamine [2-(O-chlorophenyl)-2-(methylamino)-cyclohexanone], a nonnarcotic analgesic, is a phenylcyclohexylamine derivative consisting of its two optical enantiomers, (S)- and (R)-ketamine[1]. Due to its short half-life, quick onset, lack of clinically significant respiratory depression and the possibility of inhalation to maintain the anesthetic state[2–4], it is used clinically as an anesthetic in human and veterinary medicine. However, ketamine can cause the emergence of delirium, which consists of hallucinations and an altered sensory state[5], leading to recreational misuse in clubs and drug-facilitated sexual assault[6]. Therefore, ketamine is also classified as a Schedule III substance by the US Food and Drug Administration and as a Class B drug in the UK owing to its putative addiction liability[7]. There has been an apparent increase in the use of ketamine as a drug of abuse (party drug) globally in recent years[8], which increases the challenge in the detection of cases related to ketamine abuse.

To date, there have been many studies on the mechanisms[9], metabolism[4], pharmacokinetics[10,11], and detection[12–15] of ketamine. However, few studies have investigated the time interval following ketamine abuse. Inference of the time interval following drug abuse is a challenging issue in forensic science. It can provide strong clues to the location of the suspect's drug use, the situation of the person who committed the joint crime, and even the location of the drug trafficking den. The inferences of time intervals, in some rapid deaths, depend on witnesses, police reports and the circumstances surrounding the death[16,17]. Although useful, such studies are limited in their ability to determine survival times, as many overdose deaths occur without witnesses[18]. Additionally, detecting the metabolites of drugs may be a popular choice for estimating the time of death or time of drug use. For example, in a heroin-related death, the presence of $O^6$-monoacetyl morphine in the blood may indicate a more rapid death, typically less than 20–30 min in a minority of cases[17]. The time interval following drug use can also be inferred through forensic toxicology. Our group used the blood concentration ratio of ethyl glucuronide (EtG) to ethyl sulfate (EtS) to estimate the length of time after drinking alcohol, with an error mostly lower than

[1]School of Forensic Medicine, Shanxi Medical University, Jinzhong 030600, Shanxi, China. [2]Shanxi Key Laboratory of Forensic Medicine, Jinzhong 030600, Shanxi, China. [3]Key Laboratory of Forensic Toxicology of Ministry of Public Security, Jinzhong 030600, Shanxi, China. [4]Centre for Forensic Science, University of Technology Sydney, Ultimo, NSW 2007, Australia. [5]These authors contributed equally: Tao Wang and Qian Zheng. ✉email: guozhongyuan@sxmu.edu.cn; weizhiwen2000@163.com; yunkeming5142@163.com

10% within 8 h[19]. This method, however, is only suitable within a short time interval because of the relatively short window of detection for EtG (8–12 h) and EtS (5–12 h). Even if these approaches provide an exploration means to estimate the time interval since the use of drugs, they are only suitable for some well-established conditions with witnesses and specific metabolites that can be detected because individual differences, environmental conditions, and several other variables may affect the inference of the time interval since the use of drugs.

However, metabolomics, which analyses multiple changes in the global profile, seems to be more promising than traditional methods for reliably estimating the time interval since the use of drugs[20] because it can quantify time-related multiparametric metabolites in the responses of living systems to pathophysiological stimuli or genetic modifications[21], and time-series metabolomic datasets are rich[22]. In recent studies, metabolomics has revealed that the administration of ketamine causes changes in metabolites in the urine[23], brain[24], and blood[25] of rats. Changes in the levels of some metabolites are time-dependent[26]. In another study, metabolomics was used to establish a metabolic clock of five blood metabolites that accurately predicts gestational age and identifies labor onset within two, four, and eight weeks via two to three biomarkers[27]. Metabolomics data have also been used for estimating the postmortem interval (PMI) using aqueous ovine humor samples after death for up to 24 h[28]. Taurine, choline, and succinate were found to be the metabolites most significantly correlated with the PMI.

This study aimed to infer the time interval following ketamine abuse, relying on significant changes in the serum metabolites of rats over time (up to 29 days) after a single intraperitoneal (IP) injection of ketamine. Global metabolomics data were acquired by ultra-performance liquid chromatography-quadrupole-time-of-flight mass spectrometry (UPLC-Q-TOF–MS). The levels of ketamine and its metabolites in the serum of rats were measured, and short time intervals can be inferred following the use of ketamine alone. These differential time-dependent metabolites are used for the inference of long time intervals through machine learning. These significant metabolite changes may offer new insights into the biochemical processes related to ketamine. This approach would not only lead to constructive progress in drug control and drug rehabilitation but also become an irreplaceable scientific standard for more solid evidence in court fair trials and punishment of drug crimes.

## Materials and methods

### Chemicals and reagents

Ketamine was supplied by the Institute of Forensic Science Ministry of Public Security (Beijing, China). Water was purified with a Purelab Ultra Millipore filtration unit (Labtech, Villmergen, Switzerland). HPLC-grade acetonitrile (ACN) and methanol (MeOH) were purchased from Sigma−Aldrich (Buchs, Switzerland). HPLC-grade formic acid was obtained from Aladdin (Shanghai, China).

### Animals and administration

A total of 18 male and 17 female Sprague−Dawley rats (220 ± 20 g) were purchased from the Laboratory Animal Center of Shanxi Medical University, Taiyuan, China. The animal ethics approval number was SCXK (Jin) 2015–0001. The rats were housed under 12 h light/12 h dark conditions (lights on at 6:00 and lights off at 18:00). The rats were kept in the room at 24 ± 2 °C and 50–60% humidity with free access to tap water and food for one week to acclimate to the environment. Before the experiment, the diet was removed for 12 h. A subanaesthetic dose of 30 mg/kg of ketamine is regarded as a recreational dose in rodents[24]. To exclude the influence of this dose on metabolomics, a control group (n = 5, 3 male and 2 female, injected with 0.9% saline solution) and three ketamine-treated groups were established, including a low-dose group (n = 10, 5 male and 5 female, ketamine hydrochloride was dissolved in 0.9% saline and injected with ketamine at 30 mg/kg, IP), a middle-dose group (n = 10, 5 male and 5 female, injected with ketamine at 60 mg/kg, IP), and a high-dose group (n = 10, 5 male and 5 female, injected with ketamine at 120 mg/kg, IP). Blood samples (150 µL) were serially collected from the orbital venous plexus into centrifuge tubes just before drug administration and at 0.5 h, 1 h, 2 h, 4 h, 8 h, 12 h, 1 d, 2 d, 3 d, 4 d, 6 d, 8 d, 10 d, 12 d, 14 d, 17 d, 20 d, 23 d, 26 d, and 29 d after drug administration. All rats were were humanely euthanized by $CO_2$ gas exposure after the experiment. Serum was separated from blood by centrifugation at 5000 × *g* for 10 min and stored at − 80 °C until further analysis. These samples were used as the training cohort and for screening time-dependent metabolites. All animal experiments complied with the ARRIVE guidelines, were approved by the Institutional Animal Care and Use Committee of Shanxi Medical University, and were performed in accordance with the current relevant legislation in China.

In addition, 4 male rats were injected with 0.9% saline solution or ketamine (30, 60, or 120 mg/kg, IP). Blood samples (150 µL) were serially collected from the orbital venous plexus into centrifuge tubes just before drug administration and at 1 h, 12 h, 5 d, 9 d, and 15 d after drug administration. These 24 samples were included in the validation cohort.

### Sample preparation

Serum samples from the 35 rats in the training cohort were completely randomized and analyzed across 23 days. The 24 samples from 4 rats in the validation cohort were analyzed three years later. An aliquot of 500 µL of acetonitrile and 20 µL of 100 µg/mL L-2-chloro-phenylalanine (internal standard) were added to 100 µL of serum samples and centrifuged at 13,000 × *g* for 10 min after ultrasonic extraction for 30 min at 4 °C. Three hundred fifty µL of the supernatant was dried using a vacuum concentrator (Labconco 7,810,016 Acid-Resistant CentriVap®, USA). The dried samples were redissolved in aliquots of 200 µL of methanol, filtered through a 0.22 µm membrane and transferred to sample vials for UPLC-Q-TOF MS analysis. Quality control (QC) samples were obtained by pooling 10 µL of the supernatant of each sample.

## Liquid chromatography-high-resolution mass spectrometric analysis

The untargeted metabolomics data were acquired by UPLC-Q-TOF MS analysis using HPLC on an Agilent 1290 Infinity Binary HPLC system with a BEH C18 column (2.1 × 100 mm, 1.7 µm, Waters) coupled to an Agilent 6550 iFunnel quadrupole time-of-flight (Q-TOF) MS instrument (Agilent, USA) equipped with a Dual Agilent Jet Stream (AJS) electrospray ionization (ESI) source. The MS instrument was run in positive ionization mode, with a full scan from 50 to 1000 m/z mass range at 1.40 spectra/s, a MS/MS scan with a normalized collision energy of 35 V and an isolation window of 4 m/z at 4 spectra/s. The source parameters were set as follows: drying gas temperature of 200 °C, flow rate of 14 L/min, sheath gas temperature of 350 °C, flow rate of 11 L/min, and nebulizer pressure of 35 psi.

The mobile phase consisted of water with 0.1% formic acid (A), and acetonitrile with 0.1% formic acid (B) was used to conduct chromatographic separation at a flow rate of 0.3 mL/min at 4 °C. The gradient program followed the Table 1. The postrun re-equilibrium time was 2 min. The injection volume was 5 µL.

## Metabolomic data processing

For the serum samples from the 35 rats in the training cohort, characteristic peak extraction was performed by Profinder 10.0 (Agilent, USA) through automatic peak picking, filtering with the abundance higher than 5000, and alignment with the window of 2 min, finally generating CEF files. Then, the data were imported into Mass Profiler Professional (MPP, Agilent, USA), only peaks which were detected in 50% of samples in at least one group could be used for subsequent multivariate analysis, including principal component analysis (PCA) and partial least squares-discriminant analysis (PLS-DA), as well as ANOVA. Cluster analysis was achieved through Heml 1.0.3.7[29]. Differential compounds were screened by a P value < 0.05 based on the abundance of peaks at different time points.

For the validation cohort, extraction of the characteristic peaks of the differential compounds over time was performed with Molecular Feature Extractor (Agilent, USA). The samples were normalized independently from the training cohort.

## Identification of differential compounds

The identification of differential compounds relies on accurate high-resolution mass measurements of molecular ions and fragment ions. The accurate mass of the compound was calculated through the MS spectrum and its isotope pattern using MassHunter Qualitative Analysis software (version R.08.00, Agilent, USA). The result was searched against compound databases, such as the Metabolite and Tandem MS Database (METLIN), Kyoto Encyclopedia of Genes and Genomes (KEGG), the Human Metabolome Database (HMDB) and LIPID MAPS, with a mass accuracy of 5 ppm to generate a list of candidate compounds. The isotopic pattern of the molecular ions helped to determine the likely formulas. Tandem mass spectrometry (MS/MS) spectral database matches were used to match the fragment ion spectra to the candidate compounds, which was considered a level 2 identification according to the Chemical Analysis Working Group of the Metabolomics Standards Initiative[30].

## Machine learning for the inference of time intervals following ketamine use

The abundances of the identified differential compounds were subjected to machine learning algorithms to develop a prediction model for inferring the amount of time since the last ketamine use. This study used Weka (version 3.8.6, New Zealand, https://waikato.github.io/weka-wiki/), a software package with several machine learning algorithms. After comparing the different algorithms, a random forest (RF) model was constructed to infer the time interval following the use of ketamine. Ten fold cross-validation was employed to evaluate the performance of the models. The complete dataset was divided into 10 sets, and in every round, 9 sets were used for training, and 1 set was used for testing. After the classification models were selected, the models were tested for sensitivity, specificity, accuracy, and the Matthew correlation coefficient (MCC). This model was then applied to the validation cohort for prediction and verification.

## Institutional review board statement

The animal study protocol was approved by the Institute of Zoology Animal and Medical Ethics Committee of Shanxi Medical University.

| Time (min) | A (%) | B (%) |
|---|---|---|
| 0 | 98 | 2 |
| 3 | 75 | 25 |
| 5 | 70 | 30 |
| 6 | 40 | 60 |
| 8 | 40 | 60 |
| 15 | 10 | 90 |
| 18.5 | 98 | 2 |

**Table 1.** The gradient program.

## Results and discussion

### Ketamine cohort: a study of the metabolic profile of rats after a single dose of ketamine

To determine the highly dynamic metabolic changes in rats after a single dose of ketamine, we performed high-density blood sampling at 21 time points for 29 days. The dose may affect the metabolic profile in the blood of rats, so three doses (low-dose: 30 mg/kg, middle-dose: 60 mg/kg, and high-dose: 120 mg/kg) were included in the treatment groups. To exclude the effect of blood collection on the rats, control rats treated with 0.9% saline solution were also sampled simultaneously at 21 time points. After removing outliers, a total of 35 rats (low-dose: 10, middle-dose: 10, high-dose: 10, and control: 5) and 704 samples (low-dose: 205, middle-dose: 209, high-dose: 192, and control: 98) from the training cohort were analyzed using the UPLC—Q—TOF MS method for untargeted metabolomics analysis. In addition, another separate set of 4 rats (1 low-dose, 1 middle-dose, 1 high-dose, and 1 control) with 24 samples was included as the validation cohort.

A total of 2502 features were identified and quantified across 704 samples. The instrument analysis lasted for 23 days, and 85 quality control (QC) samples were included to assess the instrument stability. The abundances of these 2502 features in both the training samples and QC samples were used for principal component analysis (PCA), in which samples were reduced dimensionally and distributed on the basis of the first two principal components (Fig. 1). The relative standard deviation (RSD) of internal standard in all samples was 29.58%. The QC samples clustered together in the score plot, indicating that the stability of the instrument was satisfactory and that further data analysis could be continued.

### Time-dependent changes in the metabolic profiles

To clearly observe the metabolomic changes over time, the abundances of the same metabolite at the same time point at the same dose were averaged, and the QC samples were also removed to generate a new PCA score plot (Fig. 2). Samples with the same dose clustered together, and the distance among samples with the same dose was greater than the distance among samples at the same time point. It might be deduced that the dose had a greater effect on the serum metabolome of the rats than did the administration time. This research suggested that the dose of a drug should be considered when studying its influence on serum metabolomics. The metabolic profiles in all 4 groups showed a time-dependent trend: samples whose sampling time was within 4 h showed obvious separation from samples at other time points. As time progressed, the metabolic profiles gradually became closer to those of the other samples when no ketamine was administered. This result suggested that the rats might have undergone a strong stress response and metabolic disorder initially, followed by an adaptive recovery process resulting in a gradual stabilization of the metabolic profiles over time.

The observation of a similar metabolic profile separation between samples within 4 h and other samples in the control group suggested that there might be other contributing factors involved (Fig. 2a). The distance of metabolic profile separation in the control group, however, was greater than that in the three drug groups, suggesting that ketamine might alleviate the stimulation of the metabolome induced by artificial treatment during blood collection, which may be related to ketamine's clinical anesthetic effect.

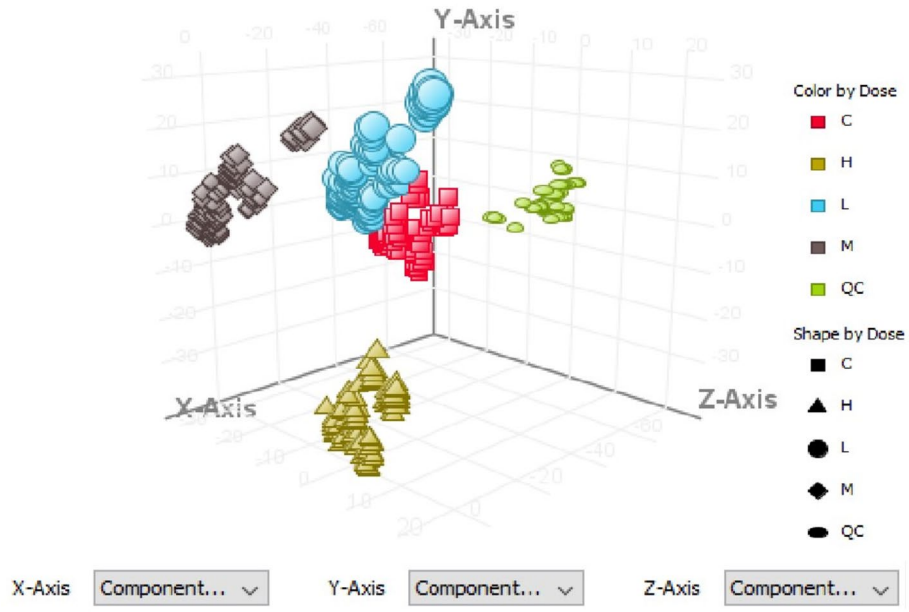


**Figure 1.** PCA score plot of metabolic patterns in rat serum. *C* control group, *H* high-dose group, *M* middle-dose group, *L* low-dose group, *QC* quality control group.

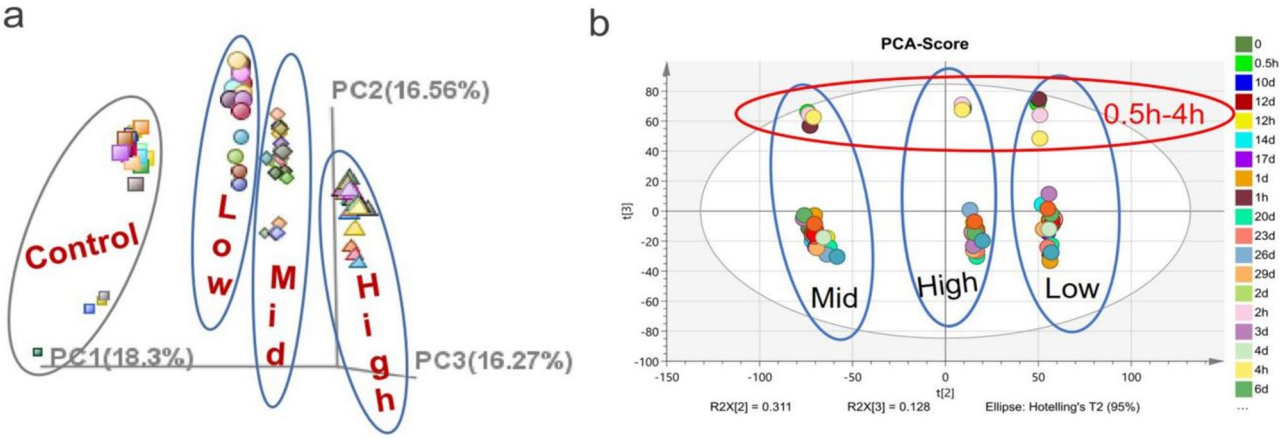


**Figure 2.** PCA score plot of metabolic patterns in rat serum. The abundance of the same metabolite at the same time point with the same dose was averaged.

## Strategies to predict the duration of a single dose of ketamine

*Ketamine and its metabolites: potential biomarkers for short intervals after ketamine administration*

The traditional method used to monitor ketamine is the detection of ketamine and its metabolites, which were also found in these untargeted metabolomics data. Ketamine is a chlorine-containing compound. Chlorine has two stable isotopes, $^{35}Cl$ and $^{37}Cl$, whose natural abundances are 75.77% and 24.23%, respectively. Chlorine-containing compounds show a characteristic distribution of chlorine isotopes that is easily recognizable via mass spectrometry. Based on these findings and mass fragmentation data, ketamine and its metabolites were detected in this study. The phase I metabolites detected included norketamine, hydroxyketamine (HK), hydroxynorketamine (HNK), and dehydronorketamine (DHNK). The phase II metabolites detected included norketamine glucuronic acid conjugate and hydroxynorketamine glucuronic acid conjugate. Combined with previous research results[1,4], the metabolic pathway of ketamine was validated in this study based on this nontargeted metabolomics analysis (Fig. 3). Ketamine is initially metabolized via nitrogen demethylation to norketamine, which is further metabolized to HNK and DHNK. HNK is formed through the hydroxylation of the cyclohexyl ring of norketamine at various locations, while DHNK is directly formed from norketamine or from HNK via a nonenzymatic dehydration event. Norketamine can also be conjugated with glucuronic acid in the serum. In addition to the major metabolic pathways of ketamine, several other pathways have also been studied. One of these pathways is the direct hydroxylation of ketamine to HK, which is readily demethylated via CYP2B6 to the corresponding HNK. HNK can also be conjugated with glucuronic acid in the serum. Because ketamine is a racemic mixture consisting of (S)- and (R)-ketamine, its nitrogen-demethylated metabolite, norketamine, is also a racemic mixture. We detected 2 chromatographic peaks corresponding to the norketamine glucuronic acid conjugate. Due to the different locations of hydroxylation, 2 peaks of HK and 3 peaks of hydroxynorketamine glucuronic acid conjugate were detected in this study. Some studies have shown that 80% of ketamine and its metabolites are excreted in the urine as conjugates of hydroxylated ketamine metabolites with glucuronic acid[4,31,32]. To the best of our knowledge, this is the first study to report the detection of the phase II metabolites of ketamine, i.e., norketamine glucuronic acid conjugates and hydroxynorketamine glucuronic acid conjugates, in blood samples. Other glucuronic acid conjugates were not detected in this study.

The relative abundances of ketamine and its metabolites were found to be dose dependent; that is, the higher the dose was, the greater the abundance was (Fig. 4). Although the trend of changes in the same metabolite in different dose groups was similar, the abundances of these metabolites peaked within 2 h. Compared with its metabolites, ketamine could be detected for the longest time—10 days. Norketamine could be detected in the serum of rats for 6 days regardless of the dosage given (Fig. 5). These metabolites could be used as indications of short time intervals following ketamine usage.

*Discovery and cluster analysis of 39 time-dependent potential biomarkers*

As Fig. 2b shows, the samples within 4 h clearly separated from samples at other time points (Fig. 2b). At the same time, ketamine could be detected within 4 h in the three ketamine groups (Fig. 4). Therefore, ketamine use within 4 h can be deduced through the detection of ketamine. Subsequent analyses were based on the data at longer time points (8 h-29 days after a single dose of ketamine). At the same time, time-dependent features obtained from the three ketamine groups were intersected to obtain biomarkers that were not influenced by dosage. There were 484, 508, and 381 differential features in the high-dose, middle-dose, and low-dose ketamine groups, respectively. There were 165 overlapping features, and 39 compounds were identified (Table S1). These 39 compounds included lipids and lipid-like molecules, ketamine and its metabolites, arachidonoyl dopamine, indole-3-acetamide and cis-2/3-dihydro-2/3-dihydroxy-4'-chlorophenyl.

The 39 compounds at all time points were used for PCA. In contrast to the plot in Fig. 2a, a PCA score plot (Fig. 6a) based on the abundance of 39 compounds showed that the samples in the control group and ketamine groups before administration (green) clustered together. The samples from the 3 ketamine groups showed a time-dependent change in the direction of principal component 1. The times were grouped from 0.5 h to 4 h

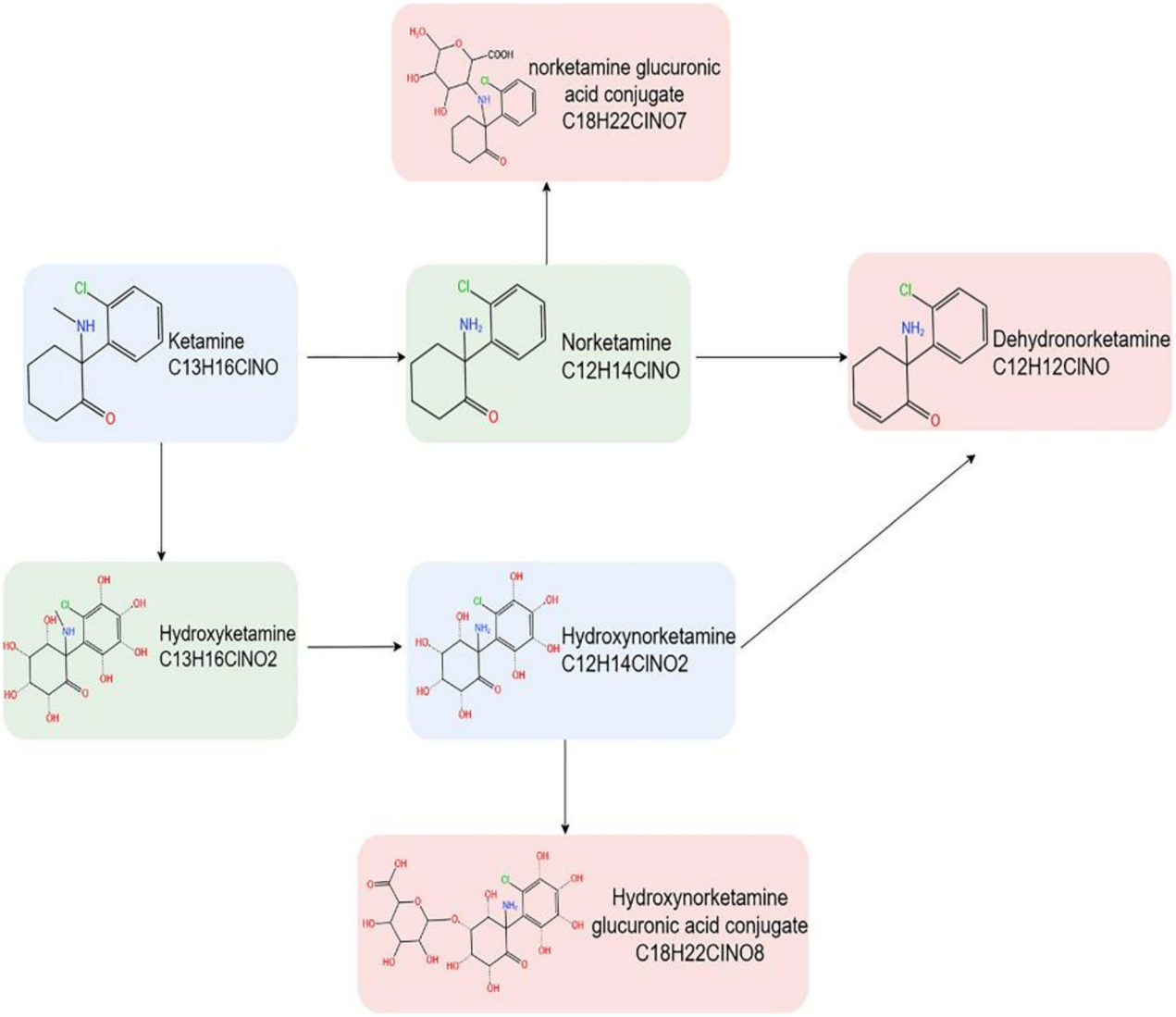


**Figure 3.** Proposed metabolic pathway of ketamine.

(blue), 8 h to 1 day (red), 2 days to 8 days (yellow), and 10 days to 29 days (azure) from left to right in Fig. 6a. The change induced by time was greater than that induced by dosage.

Cluster analysis of the fold change (average of the ketamine group/control group) of the 39 compounds revealed that ketamine and its metabolites clustered together and increased immediately when the rats were given ketamine. These compounds made the greatest contribution to the separation of the 0.5–4 h samples from the other samples (Figs. 6b and 7).

The changes in indole-3-acetamide and cis-2/3-dihydro-2/3-dihydroxy-4-chlorobiphenyl were the same as those in ketamine. These compounds could be used as potential biomarkers for recent ketamine use. Studies have demonstrated a decrease in the content of Indole-3-acetamide in rats following high-fat feeding, with a negative correlation observed with body weight[33]. Furthermore, the body weight of rats was significantly down-regulated after ketamine treatment[34], suggesting that ketamine may elevate the level of Indole-3-acetamide content to reduce body weight.

Lipids and lipid-like molecules were found to contribute significantly to the separation among longer time points after the use of ketamine (Figs. 6b and 7). Most lipids decreased after ketamine treatment, which may explain why the body weight of the ketamine group was significantly lower than that of the normal saline group reported by Wu and coauthors[34]. PC (16:1(9E)/0:0) and LysoPC (16:1(9Z)/0:0) decreased at 70% of the time points after ketamine administration compared with those in the control group, making them potential biomarkers of a single dose of ketamine. A study revealed that alterations in the levels of LysoPC and other substances were associated with the dysregulation of membrane phosphatidylcholine, leading to liver injury[35]. And in this study, LysoPC (16:1(9Z)/0:0) changed significantly, reflecting that ketamine can modify membrane phosphatidylcholine metabolism in rats and impair their hepatic function. Additionally, relevant literature has reported that ketamine can induce liver damage[36].

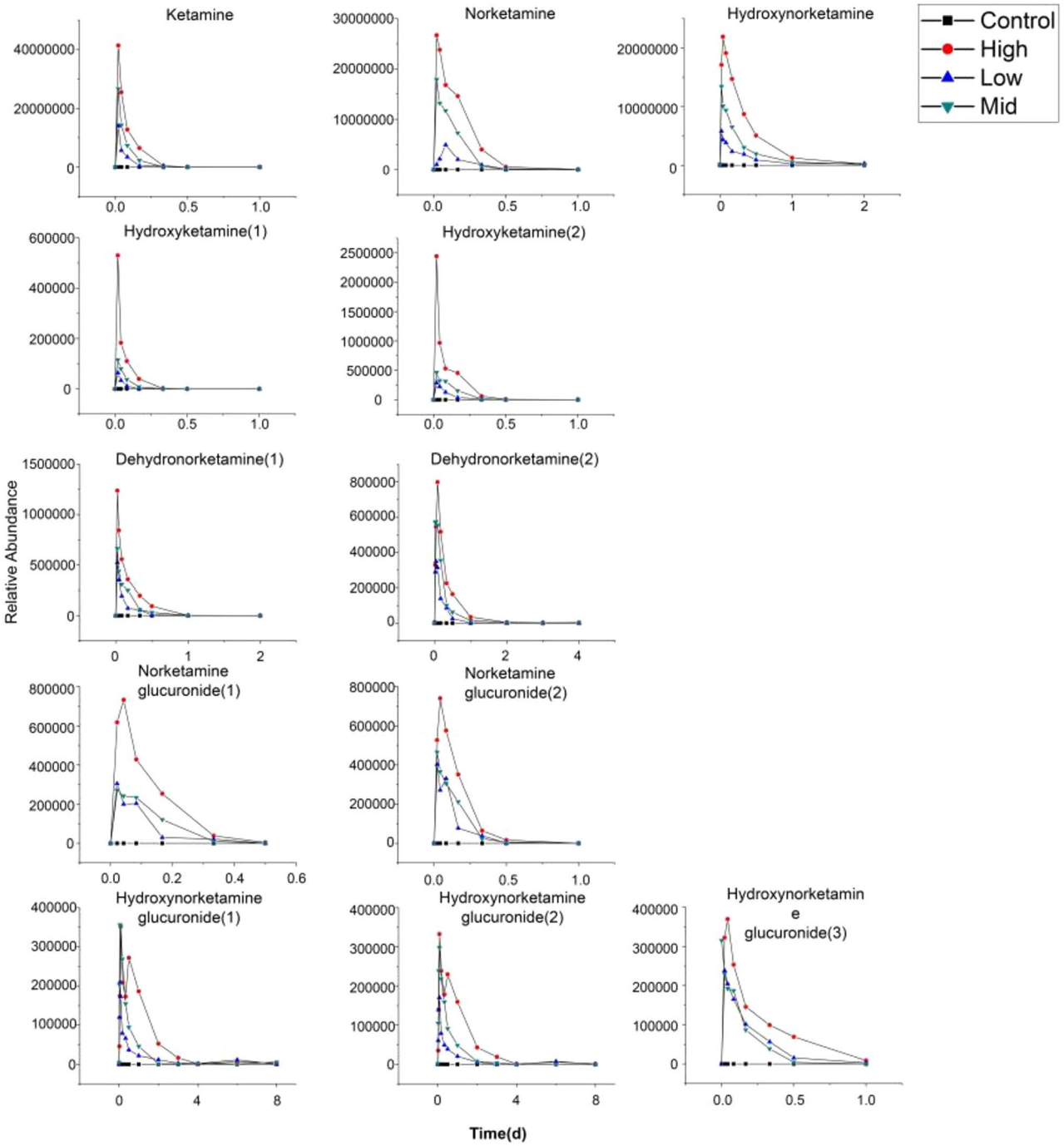


**Figure 4.** Changes in the abundance of ketamine and its metabolites over time.

*The metabolic clock of time after a single dose of ketamine determined by machine learning*

We divided all samples into five time intervals: no drug (control and before administration), 0.5 h to 4 h, 8 h to 1 day, 2 days to 8 days and 10 days to 29 days. Based on the 39 time-dependent metabolites in 704 samples from 35 rats, a model to predict the time after a single dose of ketamine was built using Weka 3.8.6. The attributes were scaled, and the random forest algorithm, which is based on the tree package, was used to construct a forest of random trees. Ten fold cross-validation was employed to evaluate the performance of the model, including the accuracy, recall, precision, false-positive rate (FPR), MCC, receiver operating characteristic (ROC) curve and area under the curve (AUC). The results of the model are shown in Table 2 and Fig. 8a. An accuracy of 85.37% and an average ROC area of 0.96 indicated high accuracy. A recall of 0.85 indicated high sensitivity. The high MCC of 0.81 indicated that the predicted model was reliable. Then, this model was used on the 24 samples in the validation set for prediction and verification. The model yielded an accuracy of 58.33% and an average ROC area of 0.81 (Fig. 8b). The lower accuracy for the validation set may be due to different sampling time points

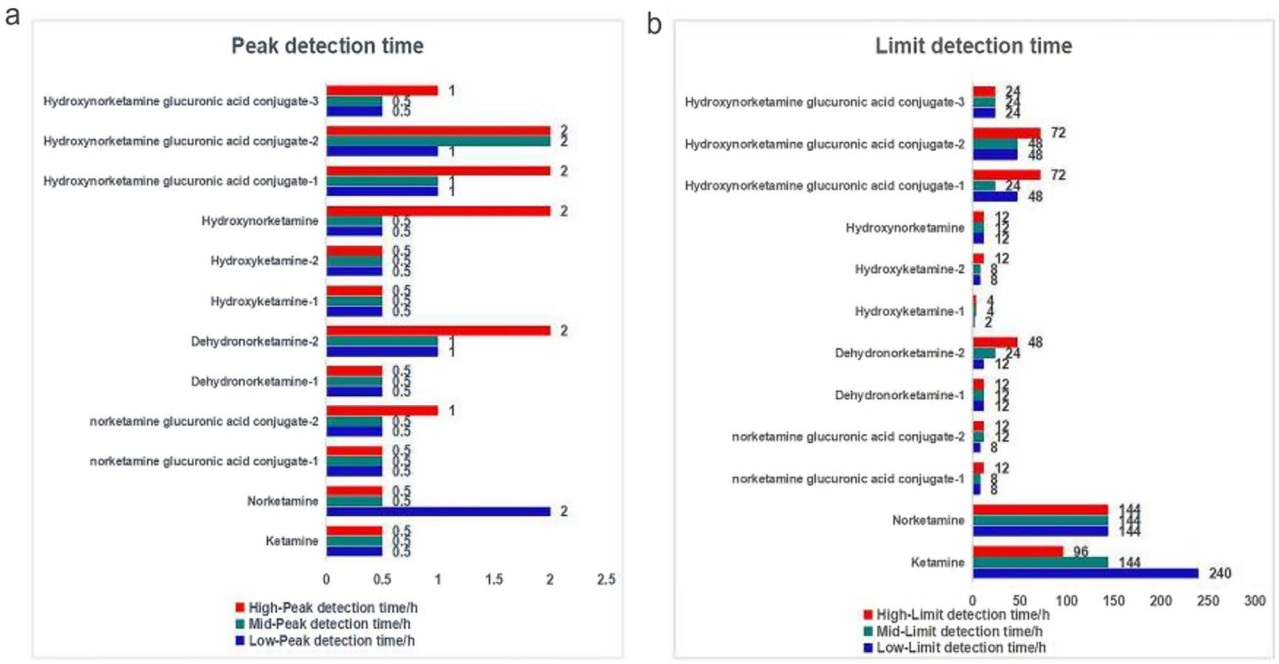


**Figure 5.** Peak and limit detection times for the abundance of ketamine and its metabolites in rat serum.

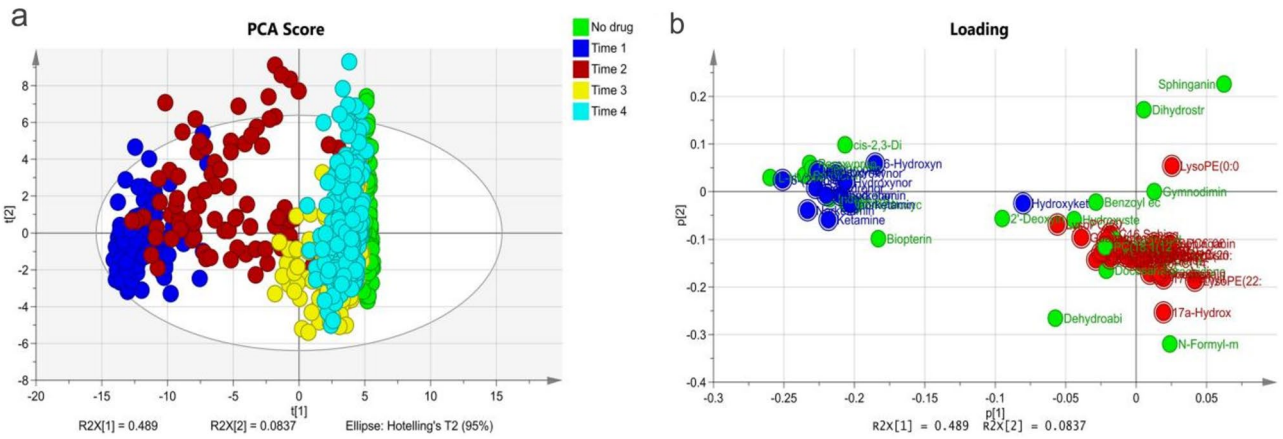


**Figure 6.** PCA model based on 66 time-dependent compounds at all time points. (**a**) Score plot. The no-drug group included samples from the control group and ketamine groups before administration (green). Time 1 included samples from 0.5 h to 4 h (blue). Time 2 included samples from 8 h to 1 day (red). Time 3 included samples from 2 to 8 days (yellow). Time 4 included samples from 10 to 29 days (azure). (**b**) PCA loading plot. Ketamine and its metabolites (red), lipids and lipid-like molecules (green), and other potential biomarkers (blue).

that were not included in the validation set. In fact, the random forest method has been utilized to construct metabolic circadian clocks in various fields. For instance, models predicting due date by measuring metabolites in the blood of pregnant women[37], metabolic clocks forecasting age by measuring metabolites in the brains of mice at different ages[38], and models estimating post-mortem interval by analyzing muscles of rats have all been developed using this approach[39]. Therefore, the random forest is a reliable method to classify samples and predict time intervals following ketamine administration. However, it is imperative to optimize this model through analysis of additional samples including human serum samples if it is to be widely applicable in practical scenarios.

## Conclusions

In conclusion, this study utilized untargeted metabolomics to detect ketamine and its metabolites in serum of rats, which could be used for estimating the time interval of ketamine usage within a short period of time (less than 4 h). A total of 39 time-dependent potential biomarkers were identified, including ketamine and its metabolites, lipids, serotonin, and other molecules. A random forest model based on these 39 potential biomarkers was established to predict the time after the last use of ketamine in rats. The accuracy of the model was 85.37% in the cross-validation set and 58.33% in the validation set. The model could potentially be used for inferring

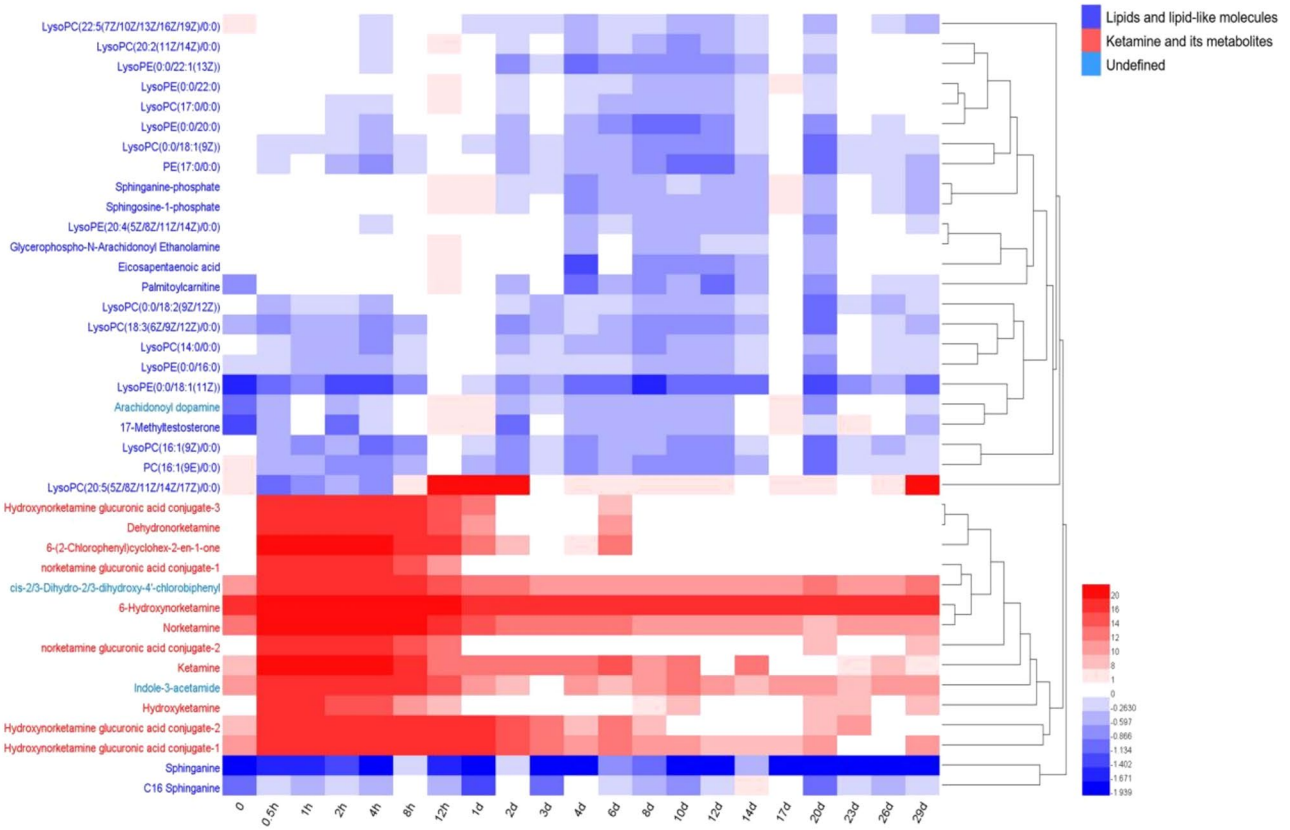


**Figure 7.** Cluster analysis of 66 characteristic time-dependent metabolites. Each row corresponds to a specific metabolite; each column corresponds to samples at the same time points. All the values are the logarithmic transformation of the fold change (average of the ketamine group/control group) of the detected abundance of each metabolite at the same time points. Red to white indicates high to intermediate relative abundance, whereas white to blue indicates intermediate to low relative abundance. Red indicates that the fold change was greater than 1.2, indicating that the abundance of metabolites increased after the IP of ketamine, while blue indicates that the fold change was less than 0.8333, indicating that the abundance of metabolites decreased after the IP of ketamine.

| | TP rate | FP rate | Precision | Recall | F-measure | MCC | ROC area | PRC area | Class |
|---|---|---|---|---|---|---|---|---|---|
| | 0.85 | 0.009 | 0.96 | 0.55 | 0.90 | 0.88 | 0.987 | 0.959 | No drug |
| | 0.97 | 0.009 | 0.96 | 0.97 | 0.96 | 0.95 | 0.996 | 0.966 | 0.5 h to 4 h |
| | 0.81 | 0.013 | 0.90 | 0.81 | 0.85 | 0.83 | 0.971 | 0.878 | 8 h to 1 day |
| | 0.68 | 0.054 | 0.77 | 0.68 | 0.72 | 0.65 | 0.927 | 0.763 | 2 days to 8 days |
| | 0.934 | 0.115 | 0.79 | 0.93 | 0.86 | 0.79 | 0.954 | 0.893 | 10 days to 29 days |
| Weighted average | 0.85 | 0.053 | 0.86 | 0.85 | 0.85 | 0.81 | 0.96 | 0.889 | |

**Table 2.** Detailed accuracy by random forest in ten fold cross validation.

time intervals up to 29 days following a single dose of ketamine. Untargeted metabolomics proved to be a valuable tool for investigating drug metabolic pathways and estimating the time interval of ketamine use based on changes in the global metabolic profile of the body. These significant metabolite changes may offer new insights into the biochemical processes related to ketamine. The development of such an analytical tool for inferring the time interval following ketamine use would benefit the process of drug control and drug rehabilitation as well as assist in ensuring fair trials and appropriate punishment for drug-related crimes within court proceedings.

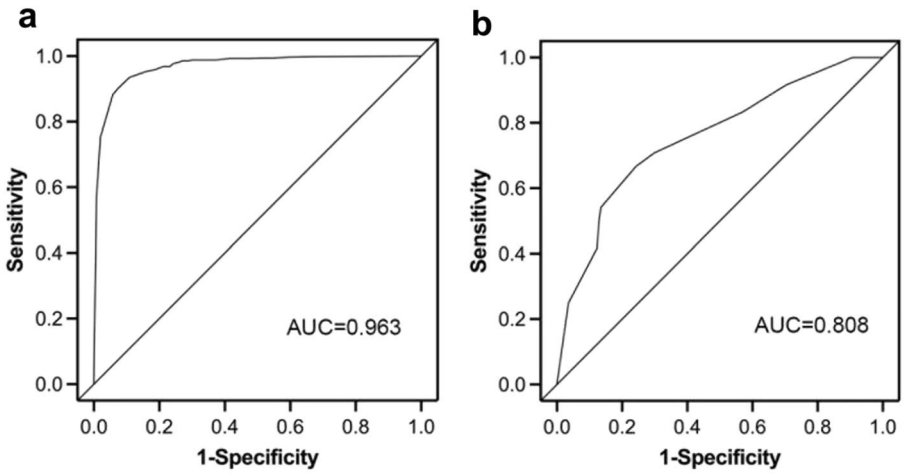


**Figure 8.** ROC curve. (**a**) ten fold cross validation. (**b**) Validation set.

## Data availability

The datasets used and/or analyzed during the current study are available from the corresponding author on reasonable request.

Received: 25 November 2023; Accepted: 8 August 2024
Published online: 14 August 2024

## References

1. Zanos, P. *et al.* Ketamine and ketamine metabolite pharmacology: Insights into therapeutic mechanisms. *Pharmacol. Rev.* **70**, 621–660. https://doi.org/10.1124/pr.117.015198 (2018).
2. Clements, J. A., Nimmo, W. S. & Grant, I. S. Bioavailability, pharmacokinetics, and analgesic activity of ketamine in humans. *J. Pharm. Sci.* **71**, 539–542. https://doi.org/10.1002/jps.2600710516 (1982).
3. Gorlin, A. W., Rosenfeld, D. M. & Ramakrishna, H. Intravenous sub-anesthetic ketamine for perioperative analgesia. *J. Anaesthesiol. Clin. Pharmacol.* **32**, 160–167. https://doi.org/10.4103/0970-9185.182085 (2016).
4. Dinis-Oliveira, R. J. *Metabolism and metabolomics of ketamine: a toxicological approach*, **2–10**, Forensic sciences research (2017).
5. White, P. F., Ham, J., Way, W. L. & Trevor, A. J. Pharmacology of ketamine isomers in surgical patients. *Anesthesiology* **52**, 231–239. https://doi.org/10.1097/00000542-198003000-00008 (1980).
6. Smith, K. M. Drugs used in acquaintance rape. *J. Am. Pharm. Assoc.* **39**, 519–525. https://doi.org/10.1016/s1086-5802(16)30472-7 (1999).
7. Simmler, L. D. *et al.* Dual action of ketamine confines addiction liability. *Nature* **608**, 368–373. https://doi.org/10.1038/s41586-022-04993-7 (2022).
8. Sassano-Higgins, S., Baron, D., Juarez, G., Esmaili, N. & Gold, M. A Review of ketamine abuse and diversion. *Depress. Anxiety* **33**, 718–727. https://doi.org/10.1002/da.22536 (2016).
9. Schwenk, E. S. *et al.* Ketamine in the past, present, and future: Mechanisms, metabolites, and toxicity. *Curr. Pain Headache Rep.* **25**, 57. https://doi.org/10.1007/s11916-021-00977-w (2021).
10. Chen, L. G. *et al.* Pharmacokinetic Interaction Study of Ketamine and Rhynchophylline in Rat Plasma by Ultra-Performance Liquid Chromatography Tandem Mass Spectrometry. *Biomed. Res. Int.* **2018**, Artn 656230910.1155/2018/6562309 (2018).
11. Kamp, J. *et al.* Pharmacokinetics of ketamine and its major metabolites norketamine, hydroxynorketamine, and dehydronorketamine: A model-based analysis. *Br. J. Anaest.* **125**, 750–761. https://doi.org/10.1016/j.bja.2020.06.067 (2020).
12. Parkin, M. C. *et al.* Detection of ketamine and its metabolites in human hair using an integrated nanoflow liquid chromatography column and electrospray emitter fritted with a single porous 10 mum bead. *J. Chromatogr. A* **1277**, 1–6. https://doi.org/10.1016/j.chroma.2012.12.019 (2013).
13. Ding, Y. *et al.* Rapid and sensitive detection of ketamine in blood using novel fluorescence genosensor. *Anal. Bioanal. Chem.* **409**, 7027–7034. https://doi.org/10.1007/s00216-017-0650-x (2017).
14. Parkin, M. C. *et al.* Detection of ketamine and its metabolites in urine by ultra high pressure liquid chromatography-tandem mass spectrometry. *J. Chromatogr.* **876**, 137–142. https://doi.org/10.1016/j.jchromb.2008.09.036 (2008).
15. Toki, H., Yamaguchi, J. I., Mizuno-Yasuhira, A. & Endo, H. Chiral LC-MS/MS method for the simultaneous determination of (R, S)-ketamine, (R, S)-norketamine, and (2R,6R;2S,6S)-hydroxynorketamine in mouse plasma and brain. *J. Pharm. Biomed. Anal.* **224**, 115168. https://doi.org/10.1016/j.jpba.2022.115168 (2023).
16. Darke, S., Ross, J., Zador, D. & Sunjic, S. Heroin-related deaths in New South Wales, Australia, 1992–1996. *Drug Alcohol Depend.* **60**, 141–150. https://doi.org/10.1016/s0376-8716(99)00147-7 (2000).
17. Darke, S. & Duflou, J. The toxicology of heroin-related death: Estimating survival times. *Addiction* **111**, 1607–1613. https://doi.org/10.1111/add.13429 (2016).
18. Davidson, P. J. *et al.* Fatal heroin-related overdose in San Francisco, 1997–2000: A case for targeted intervention. *J. Urban Health Bull. New York Acad. Med.* **80**, 261–273. https://doi.org/10.1093/jurban/jtg029 (2003).
19. Wang, L. *et al.* Estimating the time of last drinking from blood ethyl glucuronide and ethyl sulphate concentrations. *Sci. Rep.* **12**, 14262. https://doi.org/10.1038/s41598-022-18527-8 (2022).
20. Locci, E. *et al.* Forensic NMR metabolomics: One more arrow in the quiver. *Metabolomics* **16**, 118. https://doi.org/10.1007/s11306-020-01743-6 (2020).
21. Wu, Y., Judge, M. T., Edison, A. S. & Arnold, J. Uncovering in vivo biochemical patterns from time-series metabolic dynamics. *PloS One* **17**, e0268394. https://doi.org/10.1371/journal.pone.0268394 (2022).

22. Bouhifd, M., Hartung, T., Hogberg, H. T., Kleensang, A. & Zhao, L. Review: Toxicometabolomics. *J. Appl. Toxicol.* **33**, 1365–1383. https://doi.org/10.1002/jat.2874 (2013).
23. Wen, C. *et al.* Urine metabolomics in rats after administration of ketamine. *Drug Des. Dev. Ther.* **9**, 717–722. https://doi.org/10.2147/DDDT.S76898 (2015).
24. Chen, F. *et al.* Metabolic effects of repeated ketamine administration in the rat brain. *Biochem. Biophys. Res. Commun.* **522**, 592–598. https://doi.org/10.1016/j.bbrc.2019.11.140 (2020).
25. Zhang, M. *et al.* Serum metabolomics in rats models of ketamine abuse by gas chromatography-mass spectrometry. *J. Chromatogr. B Anal. Techn. Biomed. Life Sci.* **1006**, 99–103. https://doi.org/10.1016/j.jchromb.2015.10.037 (2015).
26. Weckmann, K., Labermaier, C., Asara, J. M., Muller, M. B. & Turck, C. W. Time-dependent metabolomic profiling of Ketamine drug action reveals hippocampal pathway alterations and biomarker candidates. *Transl. Psychiatry* **4**, e481. https://doi.org/10.1038/tp.2014.119 (2014).
27. Liang, L. *et al.* Metabolic dynamics and prediction of gestational age and time to delivery in pregnant women. *Cell* **181**, 1680-1692 e1615. https://doi.org/10.1016/j.cell.2020.05.002 (2020).
28. Locci, E. *et al.* A H-1 NMR metabolomic approach for the estimation of the time since death using aqueous humour: an animal model. *Metabolomics : Official journal of the Metabolomic Society* **15**, ARTN 7610.1007/s11306–019–1533–2 (2019).
29. Deng, W., Wang, Y., Liu, Z., Cheng, H. & Xue, Y. HemI: A toolkit for illustrating heatmaps. *PloS One* **9**, e111988. https://doi.org/10.1371/journal.pone.0111988 (2014).
30. Viant, M. R., Kurland, I. J., Jones, M. R. & Dunn, W. B. How close are we to complete annotation of metabolomes?. *Curr. Opin. Chem. Biol.* **36**, 64–69. https://doi.org/10.1016/j.cbpa.2017.01.001 (2017).
31. Reich, D. L. & Silvay, G. Ketamine: An update on the first twenty-five years of clinical experience. *Can. J. Anaest.* **36**, 186–197. https://doi.org/10.1007/BF03011442 (1989).
32. Adamowicz, P. & Kala, M. Urinary excretion rates of ketamine and norketamine following therapeutic ketamine administration: Method and detection window considerations. *J. Anal. Toxicol.* **29**, 376–382. https://doi.org/10.1093/jat/29.5.376 (2005).
33. Pang, Y. *et al.* Potential novel biomarkers in small intestine for obesity/obesity resistance revealed by multi-omics analysis. *Lipids Health Dis.* **21**, 98 (2022).
34. Wu, Z. G. *et al.* Urinary metabonomics of rats with ketamine-induced cystitis using GC-MS spectroscopy. *Int. J. Clin. Exp. Pathol.* **11**, 558–567 (2018).
35. Liu, F. *et al.* Determining the protective effects of Yin-Chen-Hao Tang against acute liver injury induced by carbon tetrachloride using 16S rRNA gene sequencing and LC/MS-based metabolomics. *J. Pharm. Biomed. Anal.* **174**, 567–577 (2019).
36. Dinis-Oliveira, R. J. Metabolism and metabolomics of ketamine: a toxicological approach. *Forensic Sci. Res.* **2**(1), 2–10 (2017).
37. Liang, L. *et al.* Metabolic dynamics and prediction of gestational age and time to delivery in pregnant women. *Cell* **181**(7), 1680–1692 (2020).
38. Ding, J. *et al.* A metabolome atlas of the aging mouse brain. *Nat. Commun.* **12**(1), 6021 (2021).
39. Li, J. *et al.* Multi-omics integration strategy in the post-mortem interval of forensic science. *Talanta* **268**(Pt 1), 125249 (2024).


## Acknowledgements

The authors would like to thank the Institute of Forensic Science Ministry of Public Security for providing ketamine.

## Author contributions

Conceptualization, Z.W. and K.Y.; Data curation, T.W., Q.Y. and F.G.; Funding acquisition, Z.W. and K.Y.; Investigation, Q.Z.; Methodology, T.W. and Q.Z.; Project administration, Z.W. and K.Y.; Software, T.W. and Q.Y.; Supervision, C.Z., Z.W. and K.Y.; Writing–original draft, T.W.; Writing–review & editing, T.W., Q.Z., H.C., M.H., Z.C., S.F., Z.G. and Z.W..All authors have read and agreed to the published version of the manuscript.

## Funding

This project was supported by the National Key Research and Development Program of China (2022YFC3300903, 2022YFC3302003), National Natural Science Foundation of China (No. 82130056, 82101980, 82072116), Shanxi Province Science Foundation (202103021224233) and Shanxi Province Science Foundation for Youths (202103021223236).

## Competing interests

The authors declare no competing interests.

## Additional information

**Supplementary Information** The online version contains supplementary material available at https://doi.org/10.1038/s41598-024-69805-6.

**Correspondence** and requests for materials should be addressed to Z.G., Z.W. or K.Y.